Study on differential transformer displacement sensors

Sulton Amirov[1], *Absaid* Sulliev[1*], *Shukhrat* Sharapov[1]

[1]Tashkent State Transport University, 1, Adilkhodjaev str., 100167 Tashkent, Uzbekistan

Abstract. This paper studies magnetic circuits of known and developed differential transformer sensors of large linear motion, which refer to circuits with special structure of magnetic resistance parameters distribution of long ferromagnetic cores and magnetic capacitance between them. It is shown that in the known sensor the distribution of the working magnetic fluxes along the length of the ferromagnetic cores has a nonlinear character, as a result of which the dependence between the output signal in the form of the electromotive force and the input linear motion of the sensor also has a nonlinear character. It was found that by selecting the law of changing the working gap between the middle and inner cores along the length of displacement of the moving measuring winding by making the middle concentric core in the form of a paraboloid of rotation, a linear distribution of the working magnetic flows along the length of the ferromagnetic cores and linearity of the transformation characteristic of the differential transformer sensor of large linear displacements are achieved.

1. Introduction

Automation of various technological processes, requiring the use of a set of primary transducers - sensors, makes it quite easy to perform labor-intensive processes, save energy resources, reduce the cost of production and improve its quality by ensuring close to optimal modes of operation of the control and management objects, both in normal and in emergency situations [1,2]. Meanwhile, one of the main obstacles to this is the lack of sensors for motion parameters (displacement, speed, acceleration, vibration, etc.) that meet modern requirements when working in extreme operating conditions with increased dustiness, humidity, significant temperature fluctuations, e t.c.

A comparative analysis of the main characteristics of the existing sensors of motion parameters shows that the most promising direction in solving the actual problem of more effective use of control and management systems is the use of differential transformer sensors (DTS), which by their properties (high reliability and stability of the characteristics in extreme operating conditions, as well as large output power) best satisfy the modern requirements of control and management systems [3, 4, 5]. However, the existing design schemes of DTS for measuring large linear displacements are practically unsuitable due to the instability of sensitivity in the entire measuring range and nonlinearity of the static characteristic. As a result, the accuracy of monitoring and control decreases, and in some cases, the system stability margin decreases. The need for more accurate and stable measurement of technological parameters of motion of the control and management systems objects puts forward the problem of developing new DTS for measuring large linear movements with improved information and technical characteristics, which explains the relevance of the research problem.

First, we investigate a magnetic circuit of the known DTS [5], used to measure large linear displacements, in order to determine the pattern of change of magnetic fluxes in the cores and the magnetic tension between them depending on the coordinate of the moving element. The structural diagram of the DTS with the corresponding designations is shown in Fig. 1.

The magnetic core of the sensor contains three coaxial cylindrical cores 1, 2, 3, with cores 1 and 3 connected at the ends by flanges 4 and 5 and cores 2 and 3 connected in the central part by ring jumper 6. The excitation winding consists of two sections 7 and 8 connected in series and in opposition. The measuring coil 9 encloses the rods 3 and can be moved along the magnetic coil by means of a non-magnetic rod 10 located inside the hollow rods. When an alternating voltage is supplied to the excitation winding, due to the constancy of the magnetic flux tubes length along the steel in the working range of movement of the moving part, a magnetic field along the length of the magnetic wire is formed in the sensor working gap.

*Corresponding author: absaid.sulliev@mail.ru

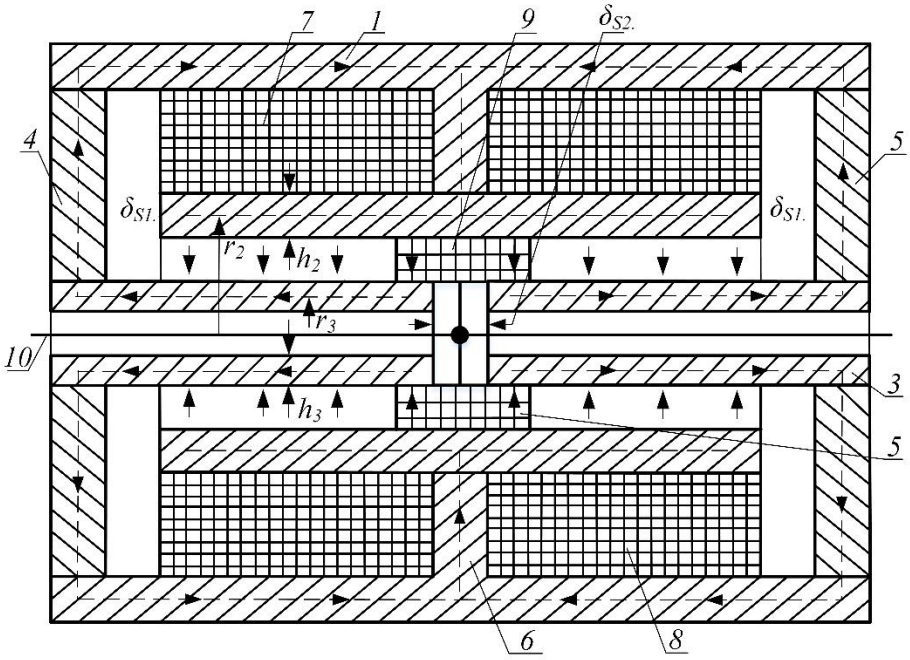

Fig.1. Design diagram of the magnetic circuit of the known DTS

2. Materials and Method

As a consequence, the output e.d.s. varies linearly as a function of the moving part movement, and the phase is constant over the moving part movement range. The phase of the output e.d.s. is reversed at zero crossing. To eliminate the influence of short-circuited body circuits on the sensor's amplitude-phase characteristics, the sensor is cut in the middle part along the generatrix. "Zero" of the sensor is adjusted by turning the covers, which changes the complex magnetic resistance of the left and right relative to the transverse axis of symmetry parts of the magnetic wire. The cylindrical body of the sensor is a shield for the magnetic fields acting in the transverse direction.

For a magnetic field acting perpendicular to the plane of the coils of the measuring coil, the presence of the gap significantly increases the resistance. In this case, the external magnetic flux is short-circuited mainly along the case.

It should be noted that in contrast to magnetic circuits of sensors with П-shaped magnetic cores, where the length of magnetic field lines along the steel throughout the length of the working gap is unequal, in the considered magnetic circuit the length of magnetic field lines along the steel throughout the length of the working gap is the same. For this reason, the former are called magnetic circuits with the usual structure of resistance and conductivity parameter distribution, and the latter, to which the investigated magnetic circuit belongs, are called magnetic circuits with the special structure of resistance and conductivity parameter distribution. Magnetic circuits with distributed parameters of all existing sensors belong either to the first group or to the second group of magnetic circuits.

In theoretical studies of magnetic circuits, we neglect the nonlinearity of steel magnetic resistance characteristics, convex fluxes at the ends of the magnetic circuit, in the area of the moving part, the measuring winding, and its longitudinal size. These assumptions do not introduce perceptible inaccuracies, but greatly simplify the calculation.

To determine the current values of magnetic voltage $U_{\mu x}$ and magnetic flux $Q_{\mu x}$, created along a long magnetic circuit by two sections of the field winding, the coordinate x of the moving part of the considered core sections 2 and 3 is most convenient to count from the central part of the magnetic circuit. Since the magnetic system is symmetrical relative to the vertical axis passing through the central part of the magnetic core, it is enough to calculate the magnetic circuit for one, for example, the left half from the central part of the magnetic core. The number in the indexes of values and parameters means that they refer to the corresponding core.

3. Results and Discussions

Changes of magnetic flux and magnetic voltage on the elementary section of magnetic circuit dx (Fig.2), created by the left section of the field winding, are found by making up the following differential equations on the basis of Kirchhoff's laws [6, 7, 8]:

$$Q'_{\mu 2x} = -U_{\mu x} C_{\mu п}, \qquad (1)$$

$$Q'_{\mu 3x} = U_{\mu x} C_{\mu п}, \qquad (2)$$

$$U'_{\mu x} = \left(Z_{\mu 3п} Q_{\mu 3x} - Z_{\mu 2п} Q_{\mu 2x}\right), \tag{3}$$

where $Z_{\mu 2п} = \frac{1}{\mu\mu_0 2\pi r_2 h_2}$, $Z_{\mu 3п} = \frac{1}{\mu\mu_0 2\pi r_3 h_3}$, $C_{\mu п} = \mu_0 \frac{\pi(r_2+r_3)}{\delta_р}$ - values of magnetic resistances of cores 2,3 and magnetic conductivity of working gap δ_r between them, per unit length of magnetic circuit; μ, $\mu_0 = 4\pi \cdot 10^{-7}\ H/m$- relative magnetic permeability of steel and magnetic constant respectively; r_2, r_3, h_2, h_3- radii and thickness of cores 2 and 3 respectively.

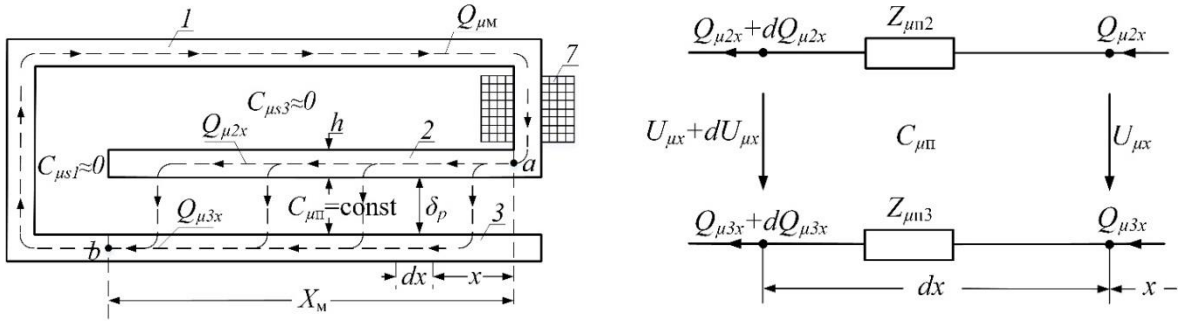

a) *b)*

Fig.2. Design diagram (a) of the left half of the magnetic circuit and the scheme of its elementary section dx (b) of the known DTS

The following equality is true for the considered magnetic circuit [6]:

$$Q_{\mu 3x} + Q_{\mu 2x} = Q_{\mu м}, \tag{4}$$

here $Q_{\mu м}$ is the total magnetic flux created by one section of the excitation winding (we neglect the scattering fluxes from the surface of core 2 to core 1 through gap δs3 and from the end parts of core 2 to flanges 4,5 through air gaps δs1 due to small values of magnetic conductivities of these gaps).

Differentiating (3) and inserting (1) and (2) into it, we obtain the following homogeneous linear differential equation of the second order:

$$U''_{\mu x} = \left(Z_{\mu 2п} + Z_{\mu 3п}\right) C_{\mu п} U_{\mu x}. \tag{5}$$

The general solution of the differential equation (5) has the following form [9]:

$$U_{\mu x} = A_1 e^{\gamma x} + A_2 e^{-\gamma x}, \tag{6}$$

where $\gamma = \sqrt{\left(Z_{\mu 2п} + Z_{\mu 3п}\right) C_{\mu п}}$is the value of the coefficient of magnetic flux propagation through the magnetic circuit, $[1/m]$; A_1, A_2- integration constants; $Z_{\mu п\Sigma} = Z_{\mu 2п} + Z_{\mu 3п}$, $[H^{-1} \cdot m^{-1}]$.

From (4) we find the magnetic flux $Q_{\mu 2x}$:

$$Q_{\mu 2x} = Q_{\mu м} - Q_{\mu 3x}. \tag{7}$$

Substituting (7) into (3), from there we find the value of magnetic flux $Q_{\mu 3x}$:

$$Q_{\mu 3x} = -\frac{1}{Z_{\mu п}} U'_{\mu x} + \frac{Z_{\mu 2п}}{Z_{\mu п\Sigma}} Q_{\mu м} =$$
$$= -\frac{\gamma}{Z_{\mu п}} A_1 e^{\gamma x} + \frac{\gamma}{Z_{\mu п}} A_2 e^{-\gamma x} + \frac{Z_{\mu 2п}}{Z_{\mu п\Sigma}} Q_{\mu м}. \tag{8}$$

The integration constants A_1 and A_2 are determined from the following boundary (boundary) conditions:

$$Q_{\mu 3x}\Big|_{x=0} = 0; \qquad Q_{\mu 3x}\Big|_{x=X_м} = Q_{\mu м}. \tag{9}$$

Substituting in (9) the boundary values of $Q_{\mu 3x}$ by (8), we obtain the following algebraic equations:

$$-\frac{\gamma}{Z_{\mu п\Sigma}} A_1 + \frac{\gamma}{Z_{\mu п\Sigma}} A_2 = -\frac{Z_{\mu 2п}}{Z_{\mu п\Sigma}} Q_{\mu м}, \tag{10}$$

$$-\frac{\gamma}{Z_{\mu п\Sigma}} e^{\gamma X_м} A_1 + \frac{\gamma}{Z_{\mu п\Sigma}} e^{-\gamma X_м} A_2 = \frac{Z_{\mu 3п}}{Z_{\mu п\Sigma}} Q_{\mu м}. \tag{11}$$

Solving together equations (10) and (11), we obtain the following values of integration constants:

$$A_1 = -\frac{Z_{\mu 2п} Q_{\mu м}}{2\gamma sh(\gamma X_м)} e^{-\gamma X_м} - \frac{Z_{\mu 3п} Q_{\mu м}}{2\gamma sh(\gamma X_м)}, \quad (12)$$

$$A_2 = -\frac{Z_{\mu 2п} Q_{\mu м}}{2\gamma sh(\gamma X_м)} e^{\gamma X_м} - \frac{Z_{\mu 3п} Q_{\mu м}}{2\gamma sh(\gamma X_м)}. \quad (13)$$

Substituting the found values of A_1 and A_2 into expressions (6) and (8), we finally have the following:

$$U_{\mu x} = -\frac{Q_{\mu м}}{\gamma sh(\gamma X_м)} \{Z_{\mu 2п} ch[\gamma(X_м - x)] + Z_{\mu 3п} ch(\gamma x)\}, \quad (14)$$

$$Q_{\mu 3x(1)} = \frac{Z_{\mu 2п} Q_{\mu м}}{Z_{\mu п\Sigma}} - \frac{Q_{\mu м}}{Z_{\mu п\Sigma} sh(\gamma X_м)} \{Z_{\mu 2п} sh[\gamma(X_м - x)] - Z_{\mu 3п} sh(\gamma x)\}. \quad (15)$$

At $Z_{\mu 2п} = Z_{\mu 3п}$ (14) and (15) takes the following form:

$$U_{\mu x} = -\frac{Q_{\mu м} Z_{\mu п\Sigma}}{\gamma sh(\gamma X_м)} \{ch[\gamma(X_м - x)] + ch(\gamma x)\}, \quad (16)$$

$$Q_{\mu 3x(2)} = \frac{Q_{\mu м}}{2} - \frac{Q_{\mu м}}{2sh(\gamma X_м)} \{sh[\gamma(X_м - x)] - sh(\gamma x)\} =$$

$$= \frac{Q_{\mu м}}{2} - \frac{Q_{\mu м} ch(0{,}5\gamma X_м)}{sh(\gamma X_м)} sh[\gamma(0{,}5X_м - x)]. \quad (17)$$

The presence of hyperbolic functions in expressions (15) and (17) already means that the dependence $Q_{\mu 3x} = f(x)$ has a nonlinear character.

In order to graph a function $Q_{\mu 3x} = f(x)$ and $U_{\mu x} = f(x)$ for ease of analysis, go to relative units:

$$Q^*_{\mu 3x(1)} = \frac{Q_{\mu 3x}}{Q_{\mu 3x = X_м}} = \frac{Z_{\mu 2п}}{Z_{\mu п\Sigma}} - \frac{1}{Z_{\mu п\Sigma} shβ} \{Z_{\mu 2п} sh[\beta(1 - x^*)] - Z_{\mu 3п} sh(\beta x^*)\}, \quad (18)$$

$$Q^*_{\mu 3x(2)} = \frac{1}{2} - \frac{ch(0{,}5\beta)}{sh(\beta)} sh[\beta(0{,}5 - x^*)], \quad (19)$$

$$U^*_{\mu x} = \frac{ch[\beta(0{,}5 - x^*)]}{ch(0{,}5\beta)}, \quad (20)$$

here $\beta = \gamma X_м$, $[-]$ is the coefficient of magnetic field attenuation in the magnetic circuit; $x^* = x/X_м$ is the coordinate value in relative units.

The function graphs $Q^*_{\mu 3x} = f(x^*)$ and $U^*_{\mu x} = f(x^*)$ are plotted at the following values of design and magnetic parameters of the investigated magnetic circuit:

$X_м = 0{,}1\ m;\ h = 0{,}005\ m;\ \delta_р = 0{,}005\ m;\ r_2 = 0{,}02\ m;\ r_3 = 0{,}03\ m;\ \mu = 1000;\ Z_{\mu 2п} = \frac{1}{\mu\mu_0 2\pi r_2 h} = 8{,}5 \cdot 10^5\ [H^{-1} \cdot m^{-1}];\ Z_{\mu 3п} = \frac{1}{\mu\mu_0 2\pi r_3 h} = 12{,}7 \cdot 10^5\ [H^{-1} \cdot m^{-1}];\ \gamma = \sqrt{(Z_{\mu 2п} + Z_{\mu 3п}) C_{\mu п}} = 9{,}1\ [m^{-1}];\ \beta = \gamma X_м = 0{,}91.$

Substituting the parameter values in (17), (18) and using the corresponding theorems for hyperbolic functions [9], we obtain the following:

$$Q^*_{\mu 3x(1)} = 0{,}4 + 27{,}96 sh(0{,}91x^*) - 9{,}91 sh(0{,}91x^*), \quad (21)$$

$$Q^*_{\mu 3x(2)} = 0{,}5 - 1{,}06 sh[0{,}91(0{,}5 - x^*)]. \quad (22)$$

$$U^*_{\mu x} = 0{,}91 ch[0{,}91(0{,}5 - x^*)]. \quad (23)$$

The graphs based on (22) and (23) show (Fig. 3), that the operating magnetic flux $Q_{\mu 3x}$ is non-linear depending on the coordinate of the moving part of the sensor and the degree of non-linearity of the function $Q^*_{\mu 3x} = f(x^*)$increases with increasing magnetic field attenuation coefficient in the magnetic circuit β, and the magnetic voltage between the cores is not constant over the moving part coordinate and the degree of non-linearity of the function $U^*_{\mu x} = f(x^*)$ also increases with increasing magnetic field attenuation coefficient in the magnetic circuit β.

Let's estimate the degree of nonlinearity of the magnetic flux distribution $Q^*_{\mu 3x}$ along the length of the cores by the following formula [7]:

$$\varepsilon = \frac{[Q^*_{\mu 3x}(x^*_1) - Q^*_{\mu 3x max} x^*_1] + [Q^*_{\mu 3x max} x^*_2 - Q^*_{\mu 3x}(x^*_2)]}{2} \cdot 100\ \% \quad (24)$$

In expression (24), the quantities x^*_1, x^*_2 are found as roots of the equation

$$\left[Q^*_{\mu 3x}(x^*)\right]' = Q^*_{\mu 3x max} = 1, \quad (25)$$

corresponding to the maximum values of positive and negative difference $Q^*_{\mu 3x}(x^*_k) - Q^*_{\mu 3x max} x^*_k$, where k=1,2.

Degrees of nonlinearity of magnetic flux distribution $Q^*_{\mu 3x}$ along the length of the cores for the cases $Z_{\mu 2п} \neq Z_{\mu 3п}$ and $Z_{\mu 2п} = Z_{\mu 3п}$, respectively, calculated by formula (24) for the above magnetic circuit parameters, for the prototype are equal:

$$\varepsilon_1 = 5{,}42\ \%\ \text{and}\ \varepsilon_2 = 2{,}73\ \%. \tag{26}$$

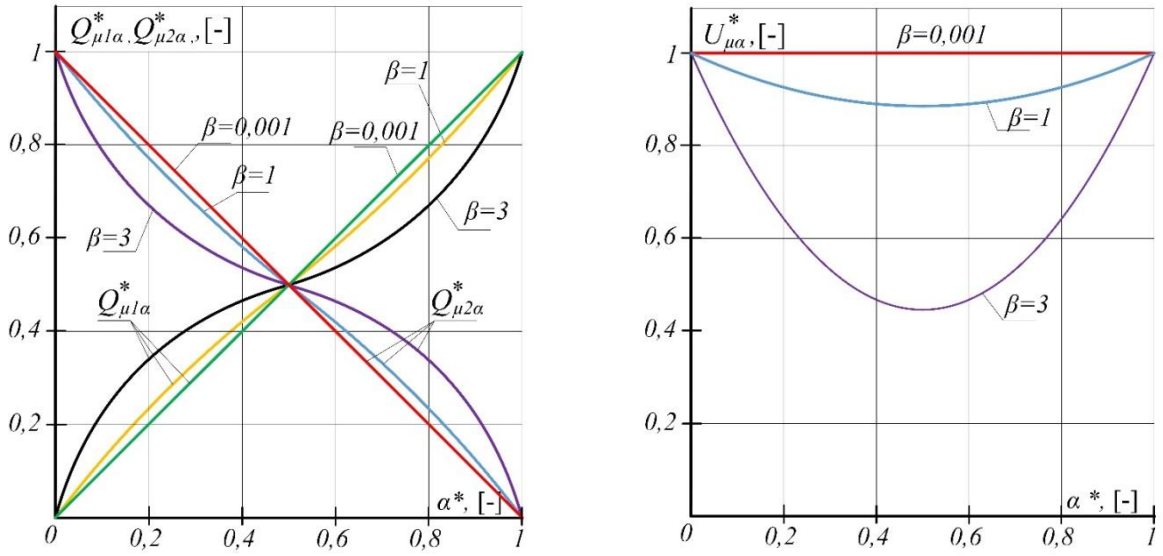

Fig. 3. Plots of the dependence of the working magnetic flux $Q_{\mu 3x}$ on the coordinate of the moving part x at different values of the magnetic field attenuation coefficient in the magnetic circuit β

Now let's obtain analytical expressions for the working magnetic fluxes in the cores and magnetic stresses between them, as well as the static characteristic of the developed DTS [10]. The structural diagram of the sensor with corresponding designations is shown in Fig. 4. The same assumptions are used here as in calculations of the magnetic circuit of the known sensor.

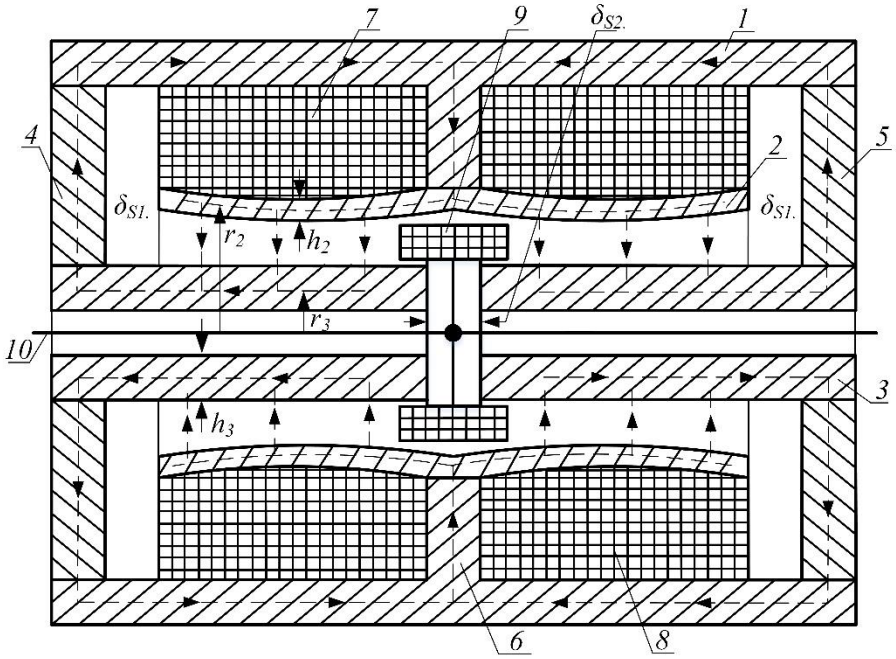

Fig. 4. Design diagram of the magnetic circuit of the developed transformer large linear displacement sensor

In order to make the displacement sensor with long cores, along the length of which the moving element in the form of a concentrated measuring winding is moving, have a linear static characteristic, it is required a linear distribution of operating magnetic flux in the range of movement of this measuring winding [7].

In the developed sensor this is achieved by selecting the law of variation of the working gap between the middle and inner cores on the length of displacement of the moving measuring winding by making the middle concentric core in the form of a paraboloid of rotation. In order to determine the law of variation of the working gap let us make and solve differential equations for the elementary section dx of the magnetic circuit, considering a linear value of magnetic conductivity of the working gap along the length of the cores to be variable, i.e. $C_{\mu\text{п}x} = var$.

The design diagram of the left half of the magnetic core of the developed DTS is shown in Fig. 5, a, and the substitution diagram of the elementary section dx of the magnetic circuit in Fig. 5, b, which differs from the substitution diagram of the elementary section dx of the magnetic circuit of the prototype (Fig. 2, b) only $C_{\mu\text{п}x}$ instead of $C_{\mu\text{п}}$.

It should be noted that in the developed sensor to create the same conditions for the passage of magnetic field lines of force across the middle and inner cores the following ratio is required:

It should be noted that in the developed sensor, in order to create the same conditions for the passage of magnetic field lines along the middle and inner cores, the following ratio is required:

$$Z_{\mu 2\text{п}} = \frac{1}{\mu\mu_0 2\pi r_2 h_2} = Z_{\mu 3\text{п}} = \frac{1}{\mu\mu_0 2\pi r_3 h_3}. \quad (27)$$

From there:

$$\frac{h_2}{h_3} = \frac{r_3}{r_2}. \quad (28)$$

Given the relation (28) we can assume that $Z_{\mu 2\text{п}} = Z_{\mu 3\text{п}} = Z_{\mu\text{п}}$.

The changes of magnetic flux and magnetic voltage on the elementary section of magnetic circuit dx (Fig. 5), created by the left section of the excitation coil, are found by composing the following differential equations on the basis of Kirchhoff's laws [8]:

$$Q'_{\mu 2x} = -U_{\mu x} C_{\mu\text{п}x}, \quad (29) \qquad Q'_{\mu 3x} = U_{\mu x} C_{\mu\text{п}x}, \quad (30)$$

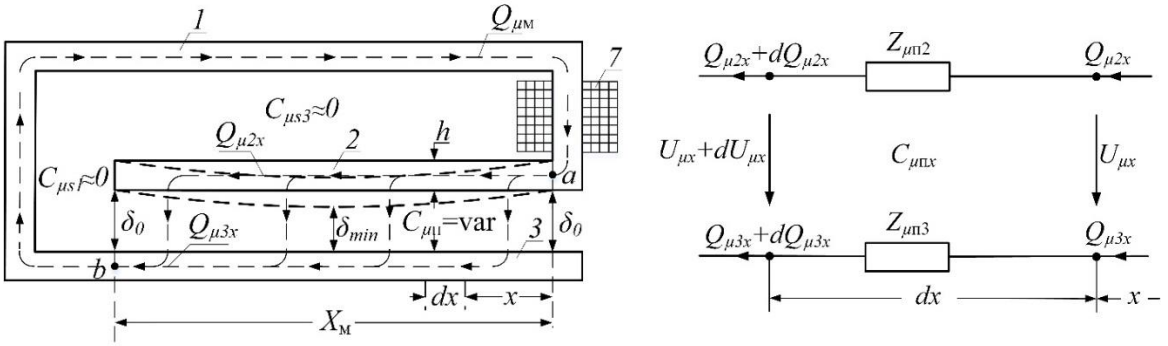

Fig. 5. Design diagram (a) of the left half of the magnetic circuit and the substitution diagram of its elementary section dx (b) of the developed DTS

$$U'_{\mu x} = Z_{\mu\text{п}}\left(Q_{\mu 3x} - Q_{\mu 2x}\right). \quad (31)$$

The condition of linearity of the distribution of the working magnetic flux $Q_{\mu 3x} = kx + b$ on the coordinate x is equality to zero of the second derivative of this function on x, i.e. $Q''_{\mu 3x} = 0$, (32). Given this condition, equation (30) takes the following form:

$$Q''_{\mu 3x} = \left(U_{\mu x} C_{\mu\text{п}x}\right)' = 0. \quad (33)$$

By integrating (33), we obtain the following:

$$U_{\mu x} C_{\mu\text{п}x} = A_1. \quad (34)$$

Differentiating (31), substituting (29), (30), and taking into account (34), we have the following differential equation:

$$U''_{\mu x} = 2U_{\mu x} C_{\mu\text{п}x} = 2A_1. \quad (35)$$

By integrating (35), we obtain:

$$U_{\mu x} = Z_{\mu\text{п}} A_1 x^2 + A_2 x + A_3. \quad (36)$$

The unit value of the magnetic conductivity of the working gap is determined from (34) with regard to (36) as:

$$C_{\mu\text{п}x} = \frac{A_1}{Z_{\mu\text{п}}\, A_1 x^2 + A_2 x + A_3} \quad (37)$$

Expressions of the magnetic fluxes $Q_{\mu 2x}$ and $Q_{\mu 3x}$, determined from (31) with regard to (4), have the following form:

$$Q_{\mu 2x} = A_1 x + \frac{1}{2Z_{\mu\text{п}}} A_2 + \frac{1}{2} Q_{\mu\text{м}}, \quad (38)$$

$$Q_{\mu 3x} = -A_1 x - \frac{1}{2Z_{\mu\text{п}}} A_2 + \frac{1}{2} Q_{\mu\text{м}}. \quad (39)$$

We obtain partial solutions of equations (36)-(39) by determining the integration constants A_1, A_2, and $A_3$for the following boundary conditions:

$$Q_{\mu 2x=0} = Q_{\mu\text{м}};\ \ C_{\mu\text{п}x=0} = C_{\mu\text{п}0} = \frac{A_1}{A_3};\ \ Q_{\mu 2x=X_\text{м}} = 0. \quad (40)$$

Substituting in (37)-(39) their marginal values according to (40), we obtain the following values of integration constants:

$$A_1 = \frac{Q_{\mu\text{м}}}{X_\text{м}};\ \ A_2 = -Z_{\mu\text{п}}\, Q_{\mu\text{м}};\ \ A_3 = \frac{Q_{\mu\text{м}}}{C_{\mu\text{п}0} X_\text{м}}\ . \quad (41)$$

Substituting (41) into (36)-(39), we obtain a layered one:

$$U_{\mu x} = \frac{Q_{\mu\text{м}}}{C_{\mu\text{п}0} X_\text{м}} \left[Z_{\mu\text{п}}\ C_{\mu\text{п}0} x^2 - Z_{\mu\text{п}}\ C_{\mu\text{п}0} X_\text{м} x + 1 \right], \quad (42)$$

$$C_{\mu\text{п}x} = \frac{C_{\mu\text{п}0}}{Z_{\mu\text{п}}\ C_{\mu\text{п}0} x^2 - Z_{\mu\text{п}}\ C_{\mu\text{п}0} X_\text{м} x + 1}. \quad (43)$$

$$Q_{\mu 3x} = \frac{Q_{\mu\text{м}}}{X_\text{м}} x, \quad (44)$$

$$Q_{\mu 2x} = Q_{\mu\text{м}} \left(1 - \frac{x}{X_\text{м}}\right) \quad (45)$$

It should be noted that the value of the magnetic flux $Q_{\mu\text{м}}$ is based on the following equation, derived from the second Kirchhoff law for a closed magnetic circuit:

$$F_\text{в} = Z_{\mu 0} Q_{\mu\text{м}} + Z_{\mu\text{п}} \int_0^{X_\text{м}} Q_{\mu 2x} dx + U_{\mu x = X_\text{м}}, \quad (46)$$

here $Z_{\mu 0}$ is the magnetic resistance of the magnetic circuit section between its points *a* and *b*.

From (46) we obtain the following value of the magnetic flux $Q_{\mu\text{м}}$:

$$Q_{\mu\text{м}} = \frac{F_\text{в}\, C_{\mu\text{п}0} X_\text{м}}{1 + Z_{\mu 0}\ C_{\mu\text{п}0} X_\text{м} + \frac{1}{2} Z_{\mu\text{п}}\ C_{\mu\text{п}0} X_\text{м}^2}. \quad (47)$$

The analysis of obtained expressions (42)-(45) shows that in order for the values of the working magnetic fluxes $Q_{\mu 2x}$ and $Q_{\mu 3x}$ to change linearly, a change in the net magnetic conductivity of the working gap between the middle and inner cores by (43) is required.

Considering that $C_{\mu\text{п}x} = \mu_0 \frac{\pi(r_2 + r_3)}{\delta_x}$, $C_{\mu\text{п}0} = \mu_0 \frac{\pi(r_2 + r_3)}{\delta_0}$ and $Z_{\mu 2\text{п}} = \frac{1}{\mu\mu_0 \pi(r_2 + r_3) h_2}$, then expression (43) takes the following form:

$$C_{\mu\text{п}x} = \mu_0 \frac{\pi(r_2 + r_3)}{\delta_0 + \frac{1}{\mu h_2}(x^2 - X_\text{м} x)} = \mu_0 \frac{\pi(r_2 + r_3)}{\delta_x}. \quad (48)$$

From (48) we can see that:

$$\delta_x = \delta_0 + \frac{1}{\mu h_2}(x^2 - X_\text{м} x). \quad (49)$$

From (47) we see that at $x = 0$ and $x = X_\text{м}$ function value $\delta_x = f(x)$ equals $\delta_{xmax} = \delta_0$, but at $x = \frac{1}{2} X_\text{м}$ - $\delta_{xmin} = \delta_0 - \frac{1}{\mu h_2} \cdot \frac{X_\text{м}^2}{2}$

The expression (47) is valid for the left and right of the central half of the magnetic wire. Therefore, for both halves of the magnetic core expression (47) can be written in the following form:

$$\delta_x = \delta_0 + \frac{1}{\mu h_2}(x^2 - X_\text{м}|x|). \quad (50)$$

For example, when $X_\text{м} = 0{,}1$ м; $h_2 = 0{,}005$ м; $\delta_0 = 0{,}01$ м and μ=1000 (value of the relative magnetic permeability of electrical steel grade 1512 when changing the induction within (0÷0,8 Tesla), which due to the large air gap in the path of the working of the magnetic flux can be assumed constant, i.e. μ=const), expression (50) has the following form:

$$\delta_x = 0{,}01 + 0{,}2(x^2 - 0{,}1|x|). \quad (51)$$

At $0 \le x \le 0{,}5X_\text{м}$ and $0{,}5X_\text{м} \le x \le X_\text{м}$ values of the function δ_x change within the limits, respectively $0{,}01 \le \delta_x \le 0{,}0095$ and $0{,}0095 \le \delta_x \le 0{,}01$. As can be seen from the last ratios, if x changes within $0 \le x \le 0{,}5X_\text{м}$ maximum variation δ_x ($\Delta\delta_{xmax} = \delta_{xmax} - \delta_{min}$) is 0,0005 м = 0,5 мм, i.e. 5% from $\delta_{xmax} = \delta_0$.

The electromotive force of mutual induction between the concentrated stationary sections 7,8 of the excitation windings and the movable measuring winding 9 is determined, according to the law of electromagnetic induction [11], as follows:

$$\dot{E}_{exit} = -\left(j\omega w_{\text{meas.}}\dot{Q}_{\mu 3x1=x} - j\omega w_{\text{meas.}}\dot{Q}_{\mu 3x2=-x}\right) = \\ = -j2\omega w_{\text{meas.}}\dot{F}_{\text{в}}\frac{C_{\mu\text{п}0}}{1+Z_{\mu 0}\ C_{\mu\text{п}0}X_{\text{м}}+\frac{1}{2}Z_{\mu\text{п}}\ C_{\mu\text{п}0}X_{\text{м}}^2}x, \quad (52)$$

here $w_{\text{meas.}}$ is the number of turns in the movable measuring winding.

4. Conclusions

Thus, the design of the developed DTS creates strictly the same magnetic resistance in the path of magnetic field lines along the whole length of the working gap due to the implementation of the linear value of magnetic capacitance of the working gap between the middle and inner cores of the magnetic core by (43), as a result of which the working magnetic fluxes are distributed along the length of the cores strictly according to linear law, and the static characteristic of the developed DTS is linear in the linear motion measurement range. In the developed detector, this is achieved by selecting the law of variation of the working gap between the middle and inner cores along the moving length of the movable measuring winding by making the middle concentric core in the form of a paraboloid of rotation.

References

1. N.R. Yusupbekov, X.Z. Igamberdiyev, A.V. Malikov, Fundamentals of process automation, Tashkent State Technical University, Tashkent (2007)
2. I.V. Miroshnik, Theory of automatic control: Linear systems, Piter, Sankt-Peterburg (2005)
3. A.V. Fedotov, Theory and calculation of inductive displacement sensors for an automatic control system, Omsk State Technical University, Omsk (2011)
4. M.Yu. Rachkov, Technical means of automation, MGIU, Moscow (2006)
5. V.G. Lukashkin, V.K. Garipov, V.V. Sleptsov, A.V. Vishnekov, Automation of measurements, control and management, Machine Building, Moskva (2005)
6. N.E. Konyuxov, F.M. Mednikov, M.L. Nechayevskiy, Electromagnetic sensors of mechanical quantities, Machine Building, Moscow (1987)
7. M.F. Zaripov, Converter with distributed parameters for automation and information-measuring technology, Energy, Moscow (1969)
8. S.F. Amirov, Sh.A. Sharapov, Mathematical Models of Displacement Measurement Differential Transformer Sensors with Different Drive Elements and Magnetic, *European Multidisciplinary Journal of Modern Science* **15**, 1-8 (2023)
9. I.N. Bronshteyn, K.A. Semendyaev, Handbook of Mathematics for Engineers and University Students, Nauka. Gl. red. Fiz.–mat. lit., Moscow (1986)
10. Yu.G. Vedmitskiy, V. V. Kukharchuk, Transient complex circuits, kirchhoff's laws and the component relations in complex-temporal form of representation, *Наукові праці ВНТУ* **1** 1-10 (2015)
11. K.S. Demirchyan, L.R. Neyman, N.V. Korovkin, V.L. Chechurin, Theoretical foundations of electrical engineering, Piter, Sankt-Petersburg (2006)
12. S. Amirov, M. Yakubov, K. Turdibekov, A. Sulliyev, Resource-saving maintenance and repair of the Traction transformer based on its diagnostics, *International Journal of Advanced Science and Technology* **29**, 1500-1504 (2020)
13. A. Sulliyev, A. Sanbetova, Sh. Kasimov, Research on Biparametric Resonant Displacement Sensors Deviation, *IOP Conf. Series Materials Science and Engineering* **883**, 012150 (2020)
14. Sh. Kasimov, A. Sulliyev, B.B. Khalkhadjayev, H.A. Kuchinov, Modern efficient technologies of oil shale mining and use in fuel and energy complex, *European Journal of Molecular & Clinical Medicine* **7**, 6279-6283 (2020)
15. S.F. Amirov, A.Kh. Sulliev, A.T. Sanbetova, I. Kurbonov, Study on the biparametrical transudations circuits with distributed parameters, *IOP Conference Series: Earth and Environmental Science* **939**, 012008 (2021)
16. K. Turdibekov, M. Yakubov, A. Sulliev, A. Sanbetova, Mathematical Models of Asymmetric Modes in High-Speed Traffic, *Lecture Notes in Networks and Systems* **247**, 1051–1058 (2022)
17. A. **Sanbetova, A. Sulliev, Sh. Kasimov,** Research on Biparametric Resonant Displacement Sensors Deviation, *IOP Conf. Ser.: Mater. Sci. Eng.* **883**, 012150 (2020)